Introduction

Distributed acoustic sensing (DAS) is an established downhole logging technique in the resource industry, initially enabling acquisition of vertical seismic profiles (VSPs) and now also microseismic data (Mizuno and Le Calvez 2023). In recent years, advances in processing technology have opened the path to using horizontally deployed DAS for seismic imaging using both reflected and refracted energy (Branston et al., 2024). And now, with the proliferation of carbon capture technology, surface DAS (S-DAS) surveys have become the focus of reservoir monitoring through time-lapse seismic imaging (Yamada et al. 2024). S-DAS has been recognized as an affordable seismic sensor for reservoir monitoring. Nevertheless, monitoring objectives extend beyond seismic imaging, and detection of induced seismicity, due to injection, is an integral part of injection monitoring. This paper compares several DAS deployment scenarios: downhole, surface, and hybrid, and contrasts the performance of such networks versus conventional geophone networks, both downhole and surface.

Microseismic Network Modelling

A 3D synthetic dynamic model was built, analogous to a Southern North Sea carbon storage location (Harrington et al. 2024), and a set of velocity and density measurements were extracted at a proposed injection site location. The data are smoothed using a 15 m Backus averaging and blocked using a 15 m minimum layer thickness criterion. The 1D model (Figure 1) is used to investigate the detectability and uncertainty of microseismic event detection at such a site using Netmod, a hydraulic fracture monitoring survey design algorithm developed by Raymer and Leslie (2011).

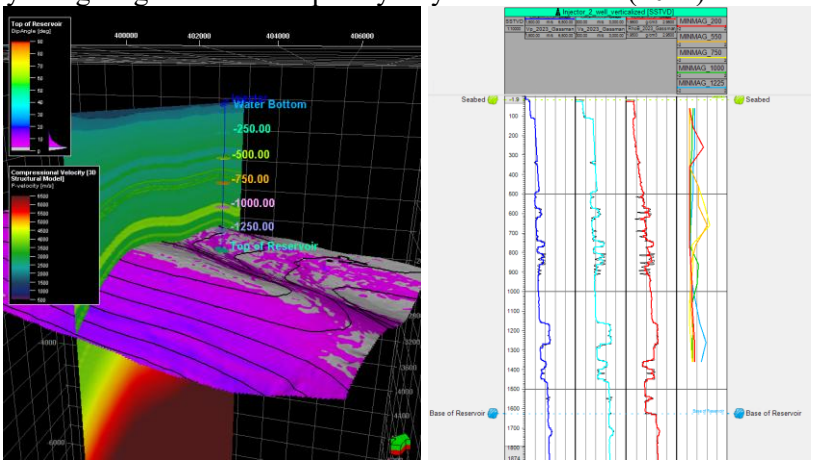

Figure 1 *Left: 3D Model built (Vp shown) with reservoir top shown (x5 vertical exaggeration, colour shows dip of reservoir in degrees); Right: Extracted compressional (blue), shear (cyan) velocities, and density (red) logs, as well as the blocked model used for 1D network modelling. The rightmost panel shows minimum detectable magnitudes along the wellbore (colour corresponds to source depth).*

The algorithm assumes a series of trial locations at regular intervals over a grid. Each trial location is evaluated numerically for a given set of sensor positions and arrival types at each station. This requires ray tracing through the velocity structure from the trial location to all the stations in the monitoring network. The workflow considers sensor geometry, sensor type source mechanism/radiation pattern, signal amplitude and path, noise and measurement uncertainty. This study focuses on the sensor geometry and type for investigation. The tested microseismic detection networks are shown in Table 1.

Array Type	Spatial Parameters	Number of Points
OBS	327 km^2	16 (3C geophones)
Downhole geophones	300 m (700–1000 m depth)	4 (3C geophones)
S-DAS star array	4 lines of 20 km length separated by 45°, injection well in the middle. Covering 314 km^2	257 points (DAS)
Downhole DAS	1240 m (70–1310 m MD)	63 (DAS)
Joint DAS	Star array and downhole DAS together	320 (DAS)

Table 1 *Induced seismicity networks tested for a conceptual CCS site in Southern North Sea.*

The attenuation is not known in the area and is assumed to be $Q_p = Q_s = 100$. Similarly, assumptions around the source mechanism are beyond the scope of this project and a spherical radiation pattern is assumed. The typical range of microseismic event magnitudes (ML) considered in monitoring, measurement, and verification (MMV) studies is -3 to 2, and this study uses ML = 2 as the magnitude of events used to investigate the uncertainty of event location. The background noise is assumed to be 10^{-6} m/s for geophones, and 10^{-9} for DAS, whilst the measurement uncertainty for time picking is 1 ms for P arrivals and 2 ms for S arrivals. For comparison, geophone hodogram uncertainty is 5° and not applicable to the DAS as it is a 1D measurement. The injection interval is 1500 m below the seabed, and the analysis area, extends 600 m above and 400 m below this target zone, although the results are shown at the top of the reservoir. The extent of the target area is 8 km x 8 km around the injection site.

Results

Permanent downhole geophones have been used in the resource industry for over 20 years (Jones and Wason 2004). A common long-life tool is deployed on tubing and has four sensor packages. Based on the 1D model, and a range of possible microseismic event depths (1225 - 250 m depths; 500 m away from wellbore), the best downhole location for the sensor network is 700–1000 m depth (Figure 1). This depth has the smallest detectable magnitudes with the least spread. In this scenario, the minimum detectable magnitude is defined as the ability to detect a microseismic event on at least one three-component geophone array. Geophone network can record events in the $-2 < M_L$ range (Figure 2, top right) with low positional uncertainty (<200 m, Figure 3) within 1.4 km at target level. For events with $M_L = 2$, the maximum distance to be detected at target level is 2.5 km. Note that due to location of this network within a wellbore, the full field coverage is limited to the area around the wellbore.

The results of network design for the ocean bottom seismometer (OBS)-type network are shown in Figure 2 (top left). In this scenario, the minimum detectable magnitude is defined as the ability to detect a microseismic event on at least one three-component OBS node. The immediate observation is that the detectability and uncertainty volumes exhibit bullseyes immediately below the sensors. This suggests that the proposed OBS-type network requires significantly more sensors (nearly twice more) to homogeneously cover the subsurface at and above the injection level. $M_L > -1.5$ is detectable but events need to be within 1 km of each sensor at target level to be detected. The maximum uncertainty (Figure 3) for events of $M_L = 2$ is more than 200 m at 1.2 km offset from any OBS sensor.

DAS networks are an emerging technology for induced seismicity monitoring. The coupling challenges associated with such networks are beyond the topic of this paper. Hence coupling is assumed to be unimpacted by operational constraints, and the performance of such a network is shown in Figure 2 (bottom right). The minimum detectable magnitude is defined as the ability to detect a microseismic event on at least three 20 m interval downhole of the DAS measurement. The detectability of the DAS network is $M_L > -1$ within 2.2 km of the injector. Due to the axial nature of the DAS measurement, maximum location (horizontal) uncertainty is high and 3D location is not possible with such scenario. To overcome this, either the instrumented wellbore needs to have a complex 3D profile or the DAS array is supplemented by additional networks on the surface. S-DAS is one such type of network.

The performance of combined, or hybrid, surface and downhole DAS networks is shown in Figure 2 (bottom row, middle). Here, the minimum detectable magnitude is defined as the ability to detect a microseismic event on at least one 20 m interval downhole and at least one 300 m surface interval on two different lines. This allows for 3D event location and the detection of events in the $-0.8 < M_L$ range within 2.8 km of the wellbore (Events in $-1<M_L<-0.8$ can be detected near the wellbore but may not be located). Maximum location uncertainty for an $M_L = 2$ is less than 20 m (Figure 3).

S-DAS networks have recently been shown to be effective at monitoring time-lapse seismic response (Bachrach et al. 2023). The performance of the star-shaped S-DAS network is shown in Figure 2 (bottom left). Here, the minimum detectable magnitude is defined as the ability to detect a microseismic

event on at least one 300 m surface interval on any three of the four lines. When comparing to the results of the joint downhole and surface DAS networks, the lack of the downhole component results in a decrease in sensitivity near the wellbore ($-0.8 < M_L$). Nevertheless, the detectability of events with $M_L \leq 2$ is homogeneous within 2.3 km of the wellbore.

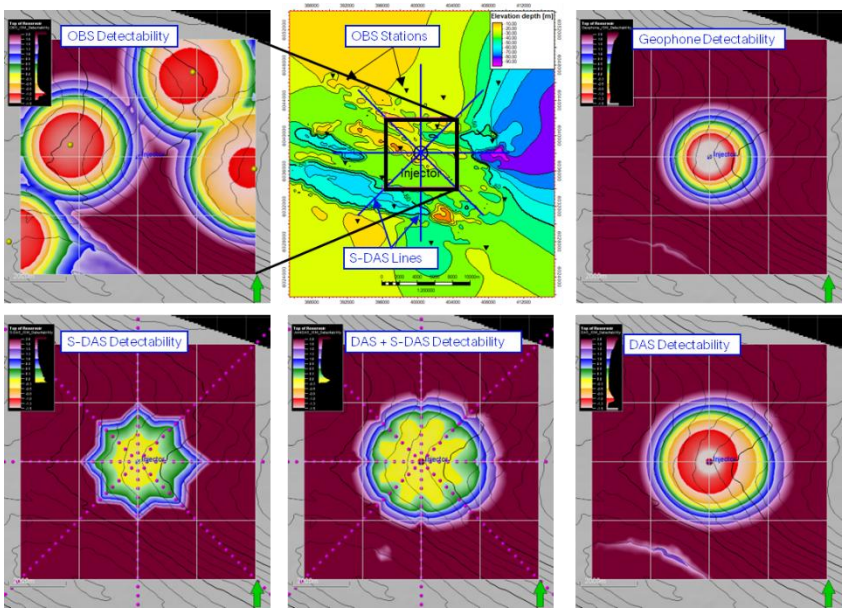

Figure 2 *Minimum detectable magnitude for various networks (each figure shows monitoring network).*

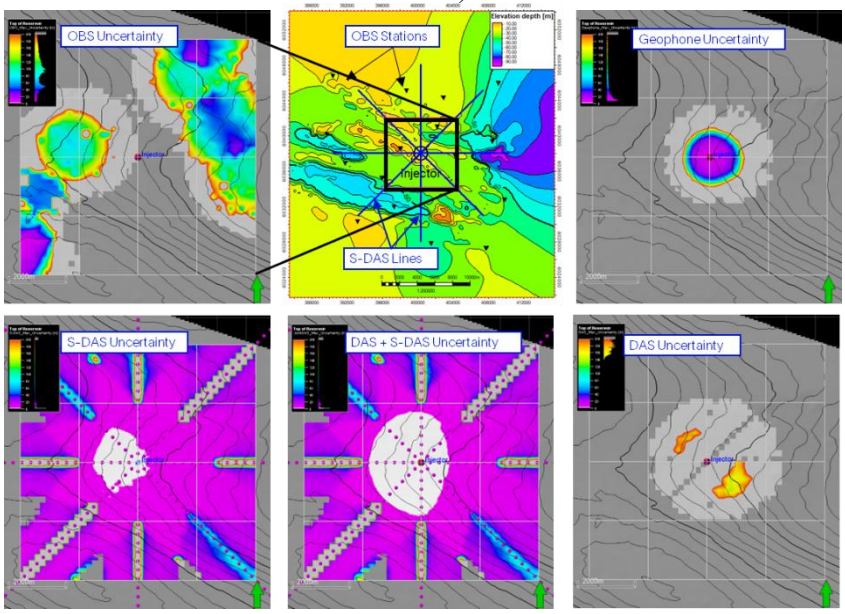

Figure 3 *Maximum event location uncertainty for various networks.*

Array Type	Detectability	200 m Uncertainty Range (km)	3D Location
Ocean bottom seismometers	$-1.5 < M_L$	1.7	YES
Downhole geophones	$-2 < M_L$	1.4	YES
Downhole DAS	$-1 < M_L$	-	NO
S-DAS + Downhole DAS	$-0.8 < M_L$	2.8	YES
S-DAS star array	$-0.8 < M_L$	2.3	YES

Table 2 *Summary of induced seismic monitoring (ISM) array performance.*

The four of the five networks compared in this study can detect and locate microseismic events below $M_L = 2$ within at least 1.4 km of the injection wellbore (Table 2). Networks deployed only within a

wellbore are limited to area around the wellbore. Networks with surface components have a larger spatial coverage. Downhole networks have a low depth uncertainty compared to surface-deployed sensors, as shown in Figures 2 and 3. It is important to note that point receivers, such as the OBS, can detect microseismic events over a large area but require a large number to do so homogeneously, even with their improved sensitivity compared to the DAS measurement. In our example, one OBS sensor is needed per 9 km^2, but this is dependent on the velocity profile and attenuation. The major benefit of OBS is its relative ease of deployment. Deployment of S-DAS is more involved than the OBS but does not require access to downhole environments and can provide real-time measurements.

Conclusions

Various induced seismicity monitoring technologies were investigated within the context of a hypothetical Southern North Sea CCS project. It was found that the combination of S-DAS and downhole DAS provides the best detectability and smallest event location uncertainty. The S-DAS network on its own also performs favorably. Nevertheless, other methodologies such as OBS and downhole geophones can provide adequate seismicity monitoring depending on local conditions. However, S-DAS networks do not require power and hence need significantly less interaction, making them an attractive and effective tool for induced seismicity monitoring.

Acknowledgements

The authors thank the Net Zero Technology Centre (NZTC) for its funding in support of this project as part of their Open Innovation Program (Spark 2368). The authors also thank SLB Multiclient for the use of the horizons used in the static and dynamic modelling as well as the model parameters.

References

Bachrach, R., Branston, M., Harrington, S., Chapelle, M., Campbell, R., and Butt, J. [2023] An introduction to cost effective geophysical CCS monitoring using fiber optic cable deployed at the surface. 4th EAGE Global Energy Transition Conference & Exhibition, Paris 2023.

Branston, M., Bachrach, R., Chapelle, M., Harrington, S., Campbell, R., and Butt, J. [2024]. Adaptive monitoring of plume migration; evaluating the potential of surface DAS. EAGE Annual Conference and Exhibition, CCS Monitoring Workshop, Oslo, Norway, June 2024.

Frignet, B., and Hartog, A. [2014] Optical Vertical Seismic Profile on Wireline Cable. SPWLA 55th Annual Logging Symposium, May 18-22, 2014.

Harrington, S., Paydayesh, M., Danchenko, D., Fletcher, A., Ackers, M., Ward, C., and Pezzoli, M. [2023] Quantifying the predicted seismic response of CO_2 injection into a depleted gas reservoir. Energy Geoscience Conference, Aberdeen, May 16th.

Jones, R., and Wason, W. [2004] PS3 – making the most of microseismic monitoring. Offshore Engineer, July 2004, pp 39-41.

Mizuno, T., Le Calvez, J. [2023] Quantitative Evaluation of DAS Passive Seismic Monitoring: Theory and Case Studies. 84th EAGE Annual Conference & Exhibition, Jun 2023, Volume 2023, p.1 - 5

Raymer, D.G., and Leslie, H.D. [2011] Microseismic Network Design - Estimating Event Detection. 73rd EAGE Conference & Exhibition, Vienna, May 2011.

Yamada, Y., Nakayama, S., Mouri, T., Lal Khaitan, M., Armstrong, P., and Podgornova, O. [2024] Imaging of multiwell and multifiber walkaway DAS-VSP datasets in a CCUS demonstration project onshore Japan. SEG Technical Program Expanded Abstracts, 503-507.